Evolution of the dust trail of comet 17P/Holmes

Gritsevich, Maria

2022-06-01

Gritsevich , M , Nissinen , M , Oksanen , A , Suomela , J & Silber , E A 2022 , ' Evolution of the dust trail of comet 17P/Holmes ' , Monthly Notices of the Royal Astronomical Society , vol. 513 , no. 2 , pp. 2201-2214 . https://doi.org/10.1093/mnras/stac822

http://hdl.handle.net/10138/345341
https://doi.org/10.1093/mnras/stac822

Monthly Notices of the ROYAL ASTRONOMICAL SOCIETY
MNRAS **513,** 2201–2214 (2022) https://doi.org/10.1093/mnras/stac822
Advance Access publication 2022 March 29

Evolution of the dust trail of comet 17P/Holmes

Maria Gritsevich [1,2,3,4]★ Markku Nissinen [2]★ Arto Oksanen [5] Jari Suomela [6] and Elizabeth A. Silber [7,8]★

[1] *Finnish Geospatial Research Institute (FGI), Vuorimiehentie 5, FI-02150 Espoo, Finland*
[2] *Finnish Fireball Network, Ursa Astronomical Association, Kopernikuksentie 1, FI-00130 Helsinki, Finland*
[3] *Department of Physics, University of Helsinki, Gustaf Hällströmin katu 2a, P.O. Box 64, FI-00014 Helsinki, Finland*
[4] *Institute of Physics and Technology, Ural Federal University, street of Peace 19, 620002 Ekaterinburg, Russia*
[5] *Hankasalmi observatory, Jyväskylän Sirius ry, Verkkoniementie 30, FI-40950 Muurame, Finland*
[6] *Clayhole observatory, Jokela, Tiriläntie 7, 05400 TUUSULA, Finland*
[7] *Department of Earth Sciences, Western University, London, ON N6A 5B7, Canada*
[8] *The Institute for Earth and Space Exploration, Western University, London, ON N6A 3K7, Canada*

Accepted 2022 March 20. Received 2022 March 17; in original form 2021 June 11

ABSTRACT

The massive outburst of the comet 17P/Holmes in 2007 October is the largest known outburst by a comet thus far. We present a new comprehensive model describing the evolution of the dust trail produced in this phenomenon. The model comprises of multiparticle Monte Carlo simulation including the solar radiation pressure effects, gravitational disturbance caused by Venus, Earth and Moon, Mars, Jupiter and Saturn, and gravitational interaction of the dust particles with the parent comet itself. Good accuracy of computations is achieved by its implementation in Orekit, which executes Dormad-Prince numerical integration methods with higher precision. We demonstrate performance of the model by simulating particle populations with sizes from 0.001 to 1 mm with corresponding spherically symmetric ejection speed distribution, and towards the Sun outburst modelling. The model is supplemented with and validated against the observations of the dust trail in common nodes for 0.5 and 1 revolutions. In all cases, the predicted trail position showed a good match to the observations. Additionally, the hourglass pattern of the trail was observed for the first time within this work. By using variations of the outburst model in our simulations, we determine that the assumption of the spherical symmetry of the ejected particles leads to the scenario compatible with the observed hourglass pattern. Using these data, we make predictions for the two-revolution dust trail behaviour near the outburst point that should be detectable by using ground-based telescopes in 2022.

Key words: methods: observational – celestial mechanics – comets: general – meteorites, meteors, meteoroids – planets and satellites: dynamical evolution and stability.

1 INTRODUCTION

During its recede from the Sun after the perihelion in 2007, comet 17P/Holmes underwent an enormous and sudden increase in brightness (Fig. 1). This unique astronomical observation has been relatively well documented. The magnitude of the comet increased from a pre-outburst value of ∼17 measured on 2007 October 23.1 (Casali et al. 2007) to 2.0 by 2007 October 25.1 (Sposetti et al. 2007; El-Houssieny, Nemiroff & Pickering 2010), which is equivalent to increase in brightness by a factor of one million (Hsieh et al. 2010). The outburst took place from 2007 October 23 to 24 (Montalto et al. 2008; Altenhoff et al. 2009; Lin et al. 2009; Sekanina et al. 2009; Hsieh et al. 2010; Reach et al. 2010; Kossacki et al. 2011; Ishiguro et al. 2013). It is the largest known outburst by a comet thus far recorded in the history of astronomical observations.

A vast amount of dust particles and gas that were ejected from the comet's coma during the outburst spread into elliptic orbits around the Sun. This phenomenon and solar radiation pressure effect on the particles were investigated by Lyytinen et al. (2013). The evolving cloud of particles widened, apparently vanishing at first. However, Lyytinen et al. (2013) re-discovered this swarm of meteoroids, which converges again at the opposite side of the Sun around the mutual (southern) node of the orbits. In one revolution the particles re-converge again at the original outburst site (referred to in this study as the near-side common node or the northern node).

Due to the differences in the orbits, a passage of the particles through any of their nodes may take up to a year or even longer. Orbital period differences of the particles cause different node arriving times and differences in orbital elements cause the hourglass shape. From purely gravitational modelling particle orbital periods can vary two years and the radiation pressure effect can lengthen orbital periods in theory to infinity for small particles (Lyytinen et al. 2013).

The increase in surface brightness of the trail of particles was expected to be sufficient to be observable in visible light. Therefore, Lyytinen et al. (2013) introduced the concept of direct observations of the ejected dust particles when they travel through the southern node situated farthest from the 2007 outburst point and later when

★ E-mail: maria.gritsevich@helsinki.fi (MG); markku.nissinen@pp.inet.fi (MN); silber@uwo.ca (EAS)

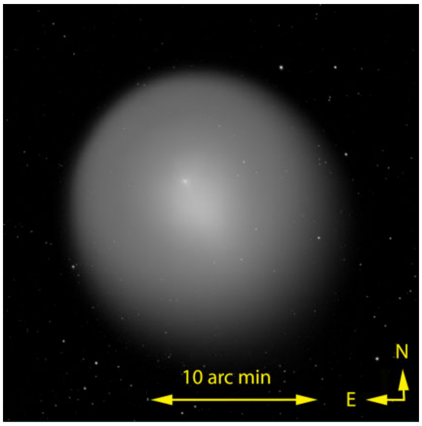

Figure 1. Comet 17P/Holmes observed at the Hankasalmi Observatory, Finland, on 2007 November 4 at 16:30:06 UT. The axes show the right ascension and declination. The compass shows north and east direction. Exposure time 60 s. Taken with SBIG ST-L-1001 CCD Camera.

they travel through the northern node situated at the 2007 outburst point itself.

In this study, we present results of the observations of the dust trail when it passes the both nodes. To the best of our knowledge, this is first direct observation of the hourglass pattern formed by the particles in the trail of a comet. Next, we present the new dust trail particle model, named the 'Dust Trail kit', implemented in Orekit, an open source space dynamics library (Maisonobe, Pommier & Parraud 2010). The basis of the model is an improved model of propagation of the particles originally developed by Esko Lyytinen, which in this work's realization is coupled with a novel approach for simulating the outburst itself. The model comprises multiparticle Monte Carlo modelling, as well as gravitational disturbance caused by Venus, Earth and its Moon, Mars, Jupiter, Saturn, and gravitational interaction of the dust particles with the comet itself. The model is validated using the observational data obtained in the dedicated campaigns described in the following section and in supplementary material. Additionally, a search was conducted for the two- revolution trail between Fall 2020 and Spring 2021. The obtained results allow us to constrain the future behaviour of the dust trail of comet 17P/Holmes when it comes close again to the 2007 outburst point.

2 THEORETICAL CONSTRAINTS AND OBSERVATIONS

The near-side common node and the far-side common node differ greatly in particle dynamics. Significantly stronger convergence of the particles occurs in the near-side node. Convergence in the far side node is not well constrained in the direction of their distance from the Sun (Lyytinen et al. 2013). Therefore, observations of the dust particles in a vicinity of the near-side node are optimal. Moreover, after two revolutions, the dust particles remain near the 2007 outburst point (Lyytinen et al. 2013).

However, in practice, observations are possible for the particles converging in the far-side node when Earth is crossing the comet's orbital plane. This occurs two times a year. Comet 17P/Holmes was previously in perihelion on 2021 February 19. It takes half a year for the comet to travel to the 2007 outburst site. Prior to that, the orbital geometry is such that the comet and its dust trail are visible simultaneously in the same telescopic field of view.

The comet itself was aligned to the top of the dust trail also when observed from Earth in 2014 September (Ishiguro et al. 2016). This

Table 1. Particle radius in mm, ejection velocity in m s^{-1} after (Reach et al. 2010) and the ratio of radiation pressure to gravity β after (Burns et al. 1979; Landgraf et al. 2000).

r, mm	Ejection velocity (m s^{-1})	β
1	330	0.0002
0.1	515	0.0022
0.01	610	0.022
0.001	640	0.280

provided a rare opportunity to observe further spatial and temporal evolution of the dust trail. Below we provide a summary of the observations made within this project and further details are given in Supplementary Material.

The first observing campaign started in February of 2013, when the comet trail passed the southern node. We used telescope.net remote controlled telescopes in the Siding Spring Observatory, Australia. The observing campaign started immediately after the observatory was opened again after an unfortunate bush fire, which destroyed the visiting centre and caused problems to network communications in the observatory and in logistics. We decided to use mainly the Planewave 500 mm Reflector with a CCD camera with Luminance filter for the observations. The image subtraction technique was used, where images taken in several nights are subtracted from each other.

For the observing campaign in the northern node that started in 2014 and continued into 2015, we used itelescope.net California, USA, and New Mexico, USA observatories with remote controlled telescopes. In California, we used the Planewave 610 mm Reflector with CCD camera and New Mexico Planewave 413 mm Reflector with CCD camera and Planewave 500 mm Reflector with CCD camera, both with Luminance filter. We also used the Hankasalmi Observatory (Finland) remote controlled telescope with CCD camera and Luminance filter in 2014 and 2015. We used the image subtraction technique but after the trail brightened significantly, the image subtraction technique was no longer required.

Our observations revealed that the particle-cloud forms a cyclic 'hourglass' pattern, which converges at specific points in space. These nodes are located where the particles' orbital planes cross each other. In the following section, we describe how we also modelled this behaviour.

3 DUST TRAIL MODELLING

The 2007 outburst process of the comet 17P/Holmes was studied in detail in the number of studies (Lin et al. 2009; Sekanina et al. 2009; Reach et al. 2010). Previous studies also detected and modelled the remnant dust cloud of comet 17P/Holmes (Ishiguro et al. 2016), as well as detected and modelled the dust cloud near the comet nucleus during the outburst (Hsieh et al. 2010).

It was proposed that the particle size can be modelled using the β parameter, which generates non-gravitational solar radiation pressure disturbance to the particle (Lyytinen et al. 2013). Ejection speed (ν) was different for different sized particles (Reach et al. 2010). Smaller particles attained greater velocities than bigger particles. We have fixed 1 mm particles to have the solar radiation pressure effect $\beta = 0.0002$ after (Burns, Lamy & Soter 1979; Landgraf et al. 2000). The particle-ejection speed relation and the corresponding β parameter relation are shown in Table 1. The list of all symbols used in our study is provided in Appendix.

We use three particle populations ranging from particulate to fine dust and referred to as follows: big (or larger) particles with 0.1–

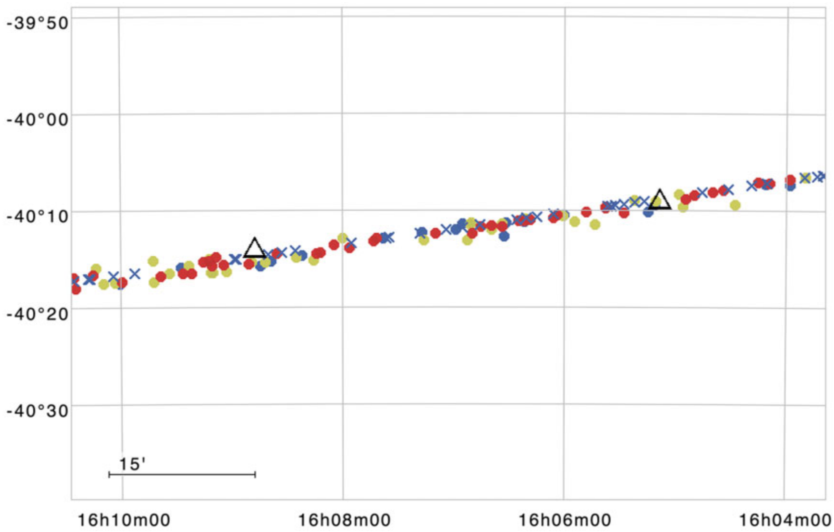

Figure 2. The 'Dust Trail kit' modelling for 2013 February 17 output is consistent with observations of (M2). X-axis shows RA and Y-axis DEC. The colour coding is used to illustrate different size particles. Blue: SPs. Yellow: MPs. Red: BPs. Black triangles: observed start and end positions of the trail. Particles ejected in the model towards the Sun are marked with crosses.

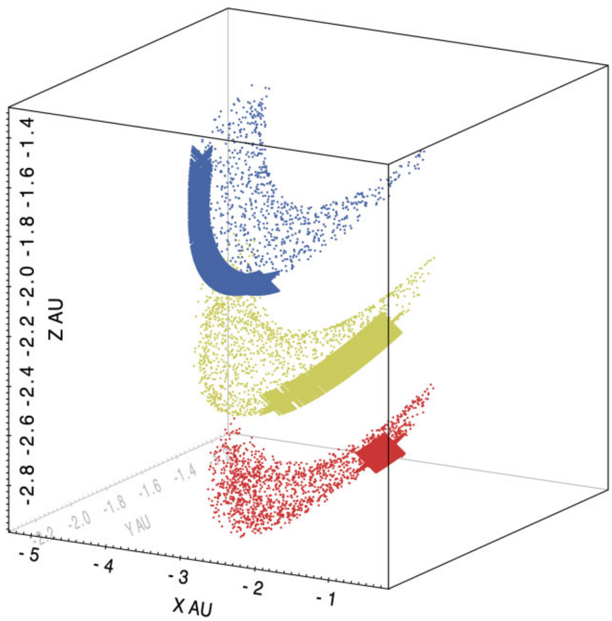

Figure 3. Modelling results for 2013 February 17 (at the time of observation M2). Particles are shown in ICRF coordinates XYZ. The colour coding used reflects the size of the modelled particles: Blue: SPs. Yellow: MPs. Red: BPs. In order to fully demonstrate all particle populations, we have applied offset Z = 0.5 to the blue particles and offset Z = −0.5 to the red particles. Particles ejected towards the Sun are marked with crosses.

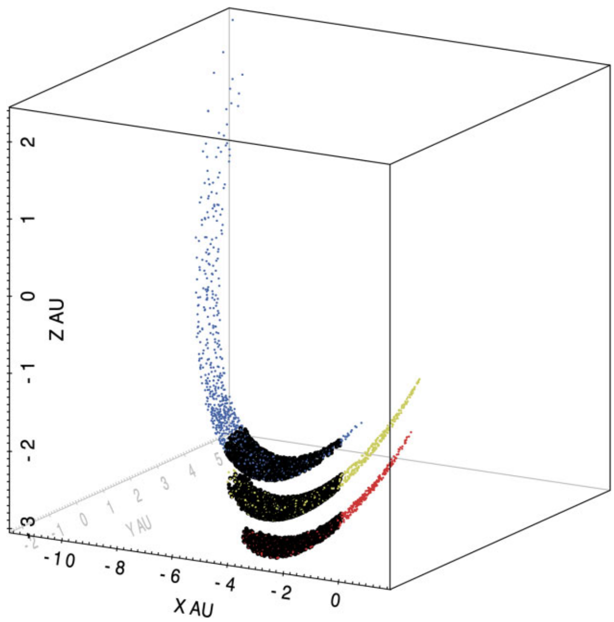

Figure 4. Modelling results for 2013 February 17 (at the time of observation M2). The particles are shown in ICRF coordinates XYZ. The colour code used reflects the size of the modelled particles: Blue: SPs. Yellow: MPs. Red: BPs. In order to fully demonstrate all particle populations, we have applied offset Z = 0.5 to the blue particles and offset Z = −0.5 to the red particles. Black circles: particles in the 40° RA window.

1 mm radius (named BPs), medium sized particles with 0.01–0.1 mm radius (MPs) and small particles with 0.001–0.01 mm radius (SPs). The distribution of the particles within each of the three groups is uniform. In the visible wavelengths range particulate dust is not observable at backscattering, at phase angles $< 30^\circ$, if it is composed of moderately or highly absorbing material (Zubko et al., 2013).

In this work, we study the particles ejected during the 2007 outburst (Sekanina et al., 2009) from the coma of 17P/Holmes by building upon, developing, and applying the earlier version of the dust trail particle model (Lyytinen, 1999; Lyytinen and Van Flandern, 2000; Lyytinen, Nissinen and Van Flandern, 2001). The new model is implemented in Orekit, which allowed us to achieve the high accuracy of computations by executing Dormad-Prince numerical integration methods with higher precision. The following considerations were added to the 'Dust Trail kit' compared to the earlier versions of the model (Lyytinen, 1999; Lyytinen and Van Flandern, 2000; Lyytinen et al., 2001; Nissinen et al. 2021a):

1) Account for gravitational disturbances caused by Venus, Earth and Moon, Mars, Jupiter, and Saturn.

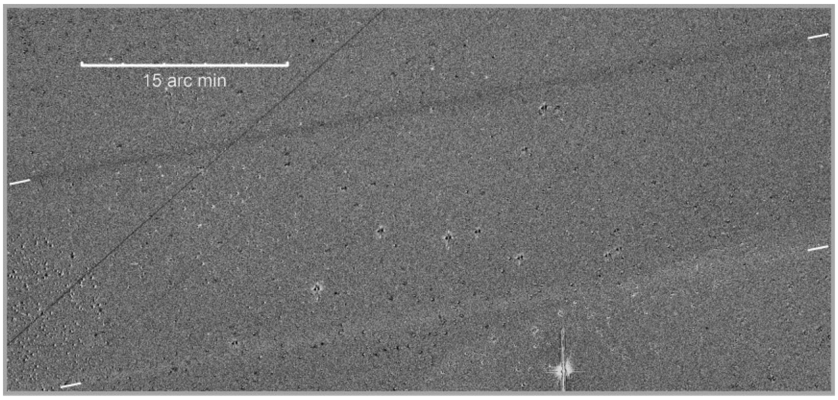

Figure 5. Observation made on 2013 February (M2). Darker trail is 17 February observation. Lighter trail is 19 February observation. Adopted from Lyytinen et al. (2013).

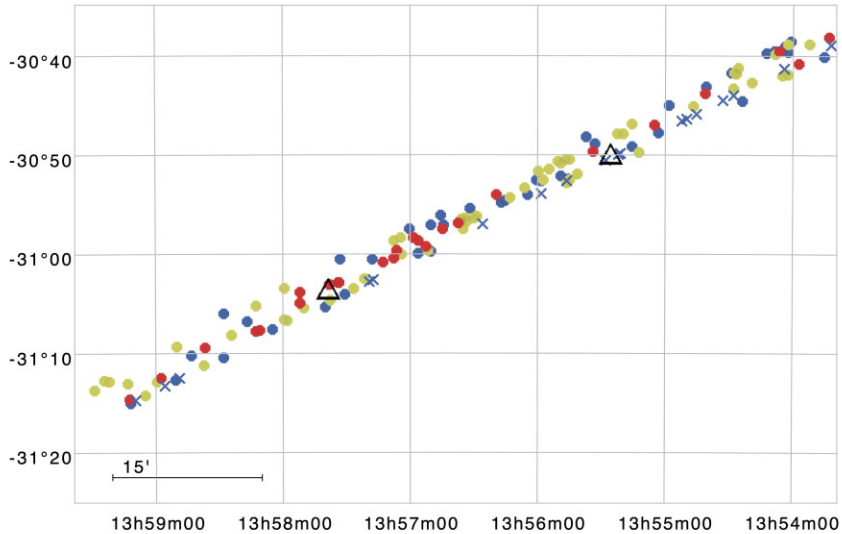

Figure 6. The 'Dust Trail kit' modelling for 2013 August 24 output is consistent with the observations of (M3). X-axis shows RA and Y-axis DEC. The colour coding is used to illustrate different size particles. Blue: SPs. Yellow: MPs. Red: BPs. Black triangles: the observed start and end positions of the trail. Particles ejected towards the Sun are marked with crosses.

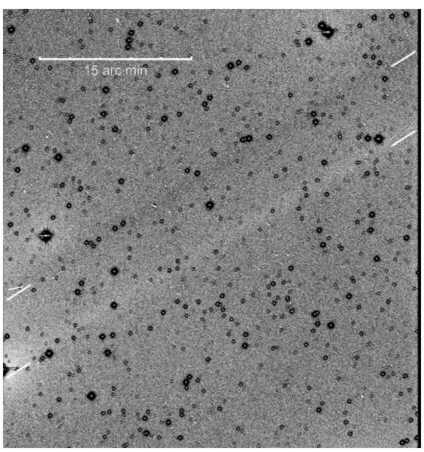

Figure 7. Observation of the 17P trail made in 2013 August 24 (M3). Image subtraction. The lighter trail is M3, see Supplementary material.

2) Inclusion of the particle's gravitational interaction with the parent comet.

3) Addition of the ejection speed section and 'particle feeding' as a one-particle-at-a-time algorithm using the Monte Carlo method.

The number of particles that can be considered in the model is arbitrary. Monte Carlo runs are accomplished with the Hipparchus add-in package to Orekit (Maisonobe et al. 2010).

We validated the model using the telescopic observations obtained from 2013 to 2015 (see details of the observations in Supplementary Material). The observations were done in both common nodes of particles' orbits (Lyytinen et al. 2013; 2014; 2015; Nissinen et al. 2021b), and are summarized in Table S1. These observations were compared to the modelled position, position angle, width of the trail and brightness fit of the observed trail as well as the modelled trail particle's integrated distribution.

Non-gravitational forces acting on the particles in a comet trail are well explained in Vaubaillon, Colas & Jorda (2005). The solar radiation pressure is the result of the electromagnetic radiation emitted by the Sun exerted upon the particles. Other active forces are the Poynting and the (diurnal) Yarkovsky-Radzievskii effects produced by the anisotropy of the thermal radiation from the particles.

Following Lyytinen (1999), Lyytinen & Van Flandern (2000), and Lyytinen et al. (2001), the non-gravitational continuous acceleration parameter in the model is set as A2 = 0. The particle ejection speed

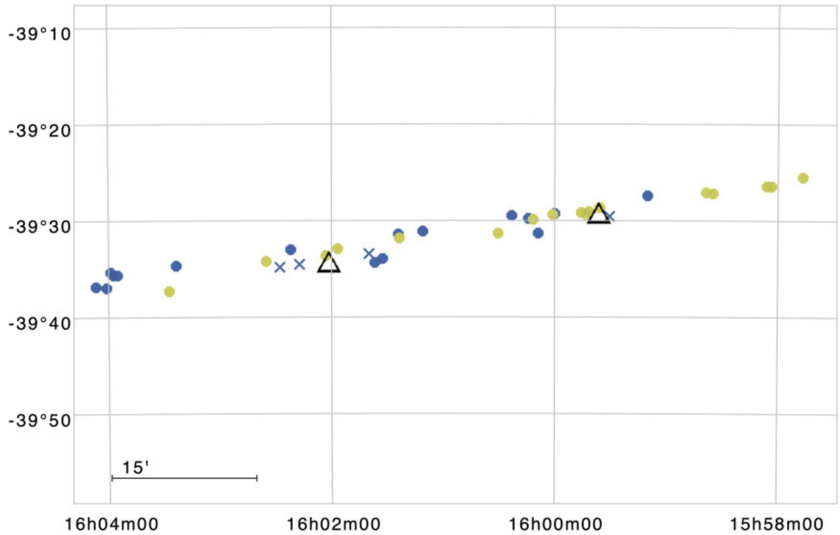

Figure 8. Modelled results of observation 2014 February 11 (M4). X-axis shows RA and Y-axis DEC. Only small and medium-sized particles are seen in the trail. Blue: SPs. Yellow: MPs. Black triangles: start and end observed positions of the trail. Our result indicates that it was possible to measure only small and medium-sized particles in the southern node. Particles ejected towards the Sun are marked with crosses.

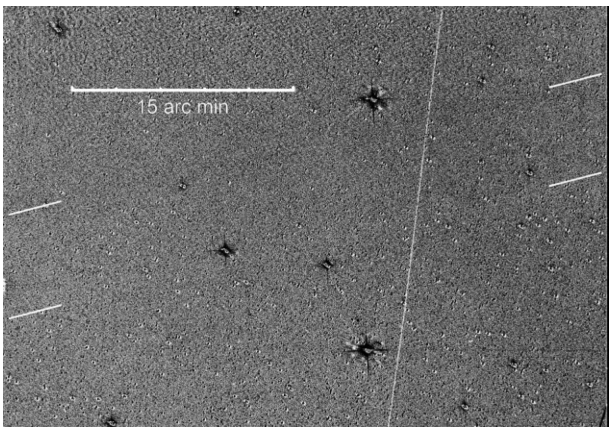

Figure 9. Observation made in 2014 February 11 (M4). Image subtraction. Upper trail is M4.

distribution is assumed to be spherically symmetric to comet's coma. The ejection speed of the 0.001 mm particles in the model is 640 m s^{-1}, which is decreased with increasing the particle size (Reach et al. 2010), Table 1.

In addition, we also modelled particles having their ejection direction (only) towards the Sun with the same physical model, the same ejection velocity distribution, and the corresponding β parameter relation.

The outburst time is not exactly known as different studies provide different, sometimes inconsistent estimates. A likely outburst date window of $t_0 = 2007$ October 23.3 ± 0.3 was given by Hsieh et al. (2010) and 2007 October 24.5 in Lin et al. (2009). The comet's starting point in our simulations was set as 2007 October 23.5.

The simulations were performed with Orekit Open Source Library for Operational Flight Dynamics in the International Celestial Reference Frame (ICRF/J2000) standard celestial reference system. The position and velocity are calculated in standard m and m s^{-1} units. The simulations are executed in variable time-steps. Spherically symmetric ejection velocity distribution is calculated using Sphere Point Picking method (Muller 1959; Marsaglia 1972). The used propagator is Runge–Kutta based Dormand-Prince integrator. The orbital elements of the comet for year 2007 are used from Giorgini (2021). Planetary and lunar locations are used as they are computed in Orekit, with the JPL Planetary and Lunar Ephemerides DE440 (Park et al. 2021).

For illustrating results of the model, the geocentric right ascension (RA) and declination (DEC) are calculated for observation time in the Earth mean equatorial coordinate system, and in the ICRF/J2000 reference frame and the coordinate system.

Based on the analysis of the expansion of the comet's coma, Hsieh et al. (2010) suggested that the outer coma was dominated by the material ejected in an instantaneous, explosive manner. In agreement with this, the 2007 outburst event is modelled as an impulse in our work. Reach et al. (2010) concluded that the outburst duration was less than 3 h and had fast event rise time and slower decay time.

As shown in Table 1, the solar radiation pressure effect described by the parameter β is effectively the particle size. The solar radiation pressure affected gravitational parameter of the Sun effective to the particle (μ') is used as an input in Orekit and it is calculated using the gravitational parameter of the Sun (μ) as described by (Burns et al. 1979):

$$\mu' = (1 - \beta)\,\mu. \tag{1}$$

The particles have a calculated location and velocity at the start of the modelling sequence. The particle ejection velocity distribution is spherically symmetric or towards the Sun and is scaled with corresponding β value. The ejection velocity is added to the particle velocity at the start location:

$$\begin{bmatrix} v_x \\ v_y \\ v_z \end{bmatrix} = \begin{bmatrix} v_{0x} \\ v_{0y} \\ v_{0z} \end{bmatrix} + \begin{bmatrix} v_{ex} \\ v_{ey} \\ v_{ez} \end{bmatrix} \tag{2}$$

When sampling the particles in the observation window and calculating RA and DEC in geocentric coordinate system, the Earth's location is subtracted:

$$\begin{bmatrix} x_{gw} \\ y_{gw} \\ z_{gw} \end{bmatrix} = \begin{bmatrix} x_p \\ y_p \\ z_p \end{bmatrix} - \begin{bmatrix} x_{\mathrm{earth}} \\ y_{\mathrm{earth}} \\ z_{\mathrm{earth}} \end{bmatrix}. \tag{3}$$

For comparing the model with the observations, the declination α and right ascension θ are calculated using Orekit. The light-time

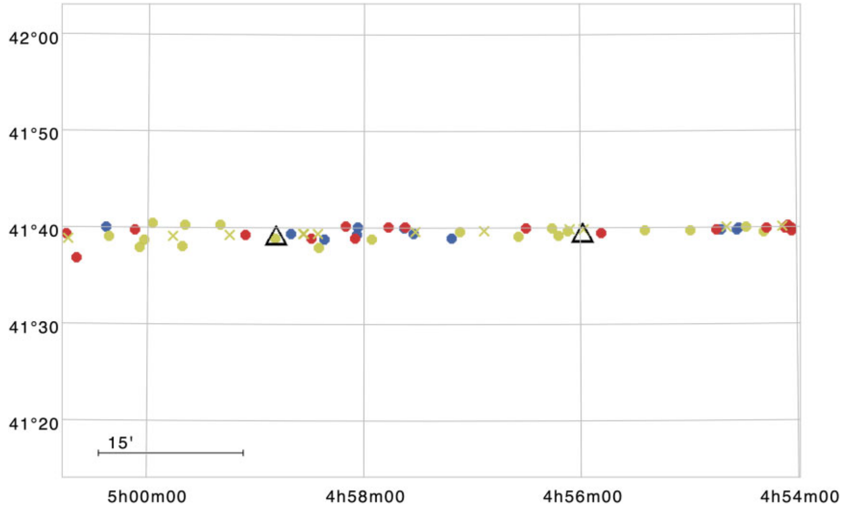

Figure 10. Modelled results of the observation made in 2014 August 27 (M5). X-axis shows RA and Y-axis DEC. Colour coding: Blue: SPs. Yellow: MPs. Red: BPs. Black triangles: start and end of the observed trail positions. Particles ejected towards the Sun are marked with crosses.

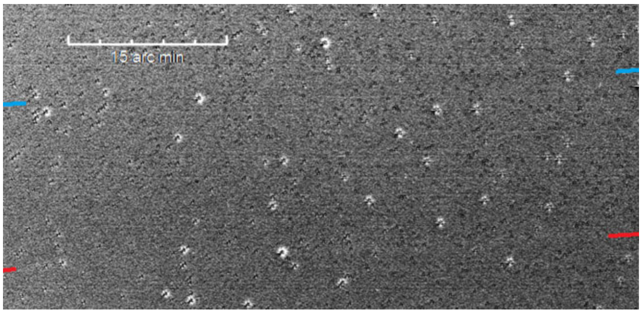

Figure 11. Observation made in 2014 August 27 (M5). Image subtraction. Lighter trail shown with the red markers is M5.

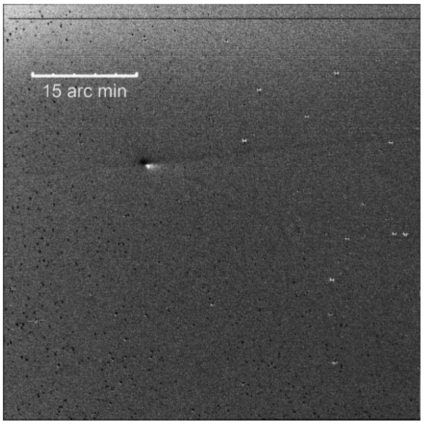

Figure 13. Image taken with the T24 telescope obtained when 17P/Holmes was aligned with the dust trail. The observation was made in 2014 September 16 (M6). Image subtraction. The darker trail is M6.

correction, i.e. the displacement in the apparent position of an object from its geometric position caused by the object's motion during the time it took the light to reach an observer, was not taken into

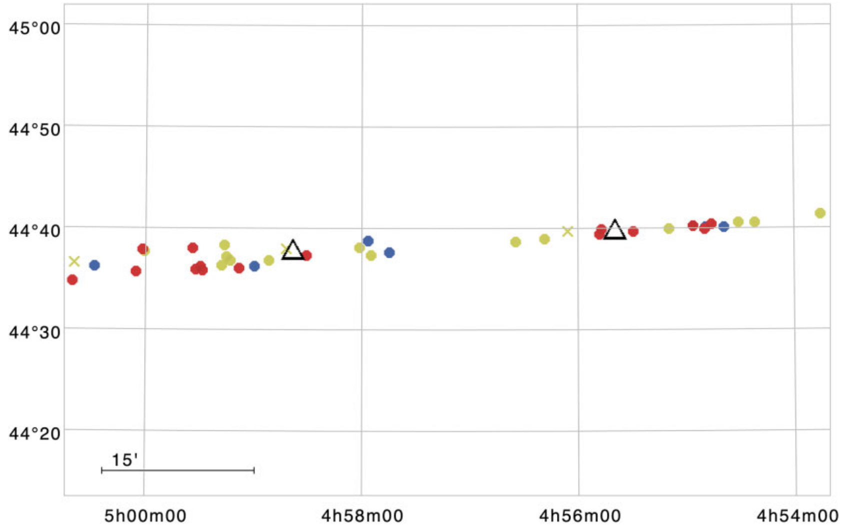

Figure 12. Modelling results versus observation made in 2014 September 16 (M6). X-axis shows RA and Y-axis DEC. Colour code of modelled particles: Blue: SPs. Yellow: MPs. Red: BPs. Black triangles: start and end observed positions of the trail. Particles ejected towards the Sun are marked with crosses.

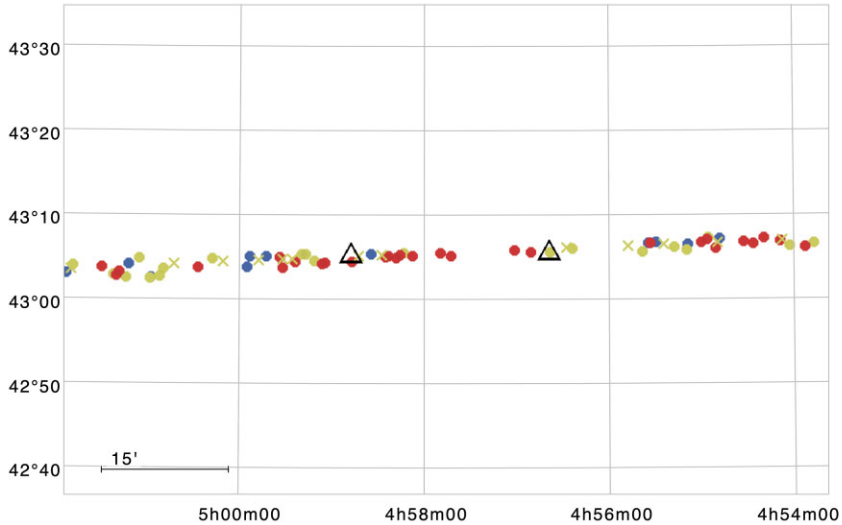

Figure 14. Modelling of the observation 2014 September 6 (M12). X-axis shows RA and Y-axis DEC. Blue: SPs. Yellow: MPs. Red: BPs. Black triangles: start and end observed positions of the trail. Particles ejected towards the Sun are marked with crosses.

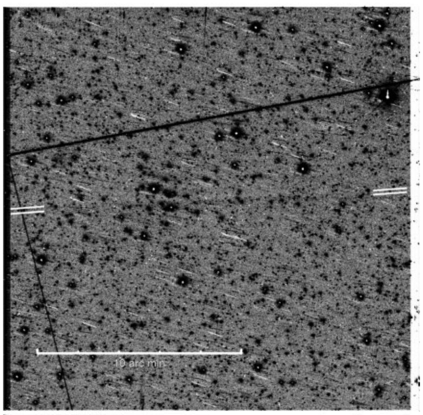

Figure 15. Observation made in 2014 September 6 (M12). Image subtraction. Lower trail is M12.

account in our calculations, although this may be a valid correction to consider (Dumoulin 1994).

The coordinates of the comet and the Earth's position are taken from the JPL Horizons system (Giorgini 2021). The trail spatial location is obtained from the dust trail model described in this section.

4 RESULTS AND DISCUSSION

A typical simulation executed in this work is run with ∼2000 particles in spherical outburst modelling and with ∼800 particles in towards the Sun outburst modelling. When compared to observations, we select particles fitting for every case via random sampling using Hipparchus package and Orekit. Our visualization selection constraint is 40° variation in RA. Because the model gives out particle coordinates with one day resolution at JD zero decimal for clarity, the observed position of the trail is corrected by adjusting the time

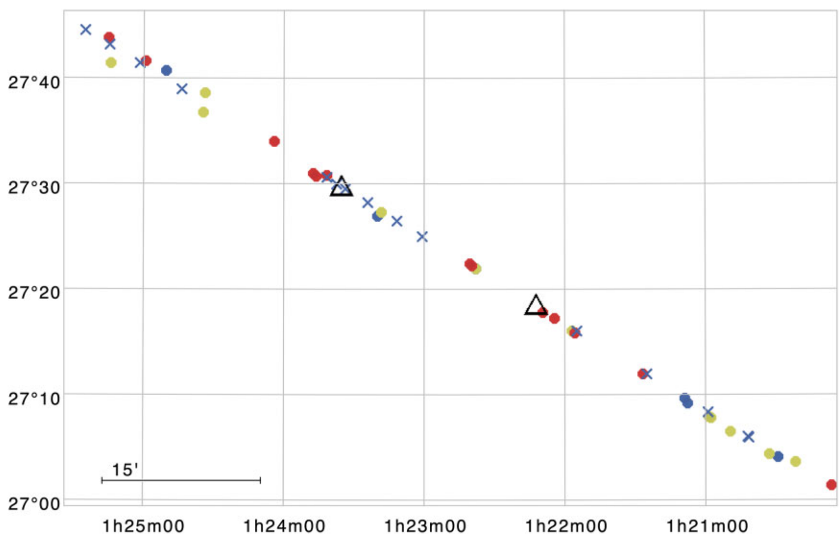

Figure 16. Modelling of observation 2015 February 14 (M13). X-axis shows RA and Y-axis DEC. Blue: SPs. Yellow: MPs. Red: BPs. Black triangles: start and end observed positions of the trail. Particles ejected towards the Sun are marked with crosses.

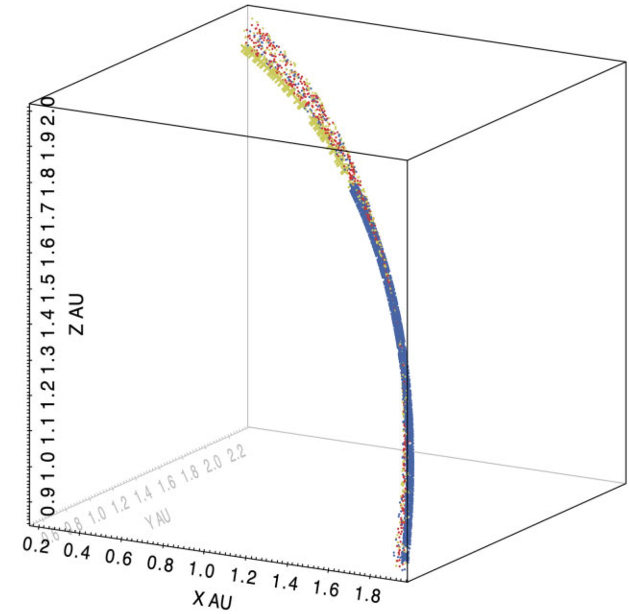

Figure 17. Modelling results versus observation made in the northern node in 2015 February 14 (M13). The particles are shown in the ICRF coordinates XYZ. Colour code stands for particle size. Blue: SPs. Yellow: MPs. Red: BPs.

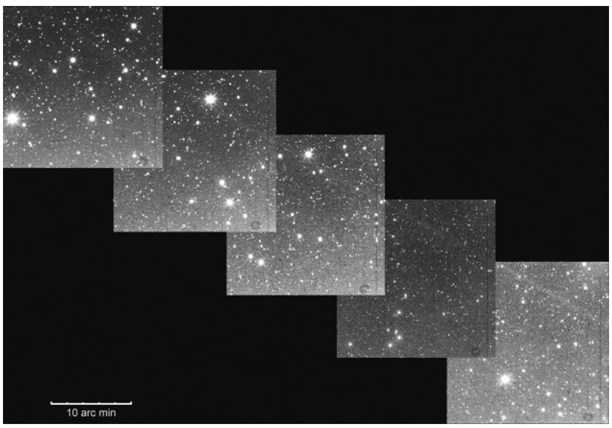

Figure 18. Observation made in 2015 February 14 (M13). No image subtraction was required.

of the observation to match the time stamp used in the modelled coordinate list (Lyytinen et al. 2013, 2014).

The gravitational interaction of particles with the comet itself is included in the new model, although in our modelling results for this kind of outburst scenario its contribution was found to be negligible.

Below we discuss comet 17P/Holmes dust trail behaviour starting from 2012.

4.1 Overall dust trail evolution from 2012 to 2021

At the beginning of 2012, the dust particles arrived near the southern node after orbiting 0.5 revolution past the 2007 outburst point. The medium sized particles arrived first, in a wide (few hundredths of AU) formation already in 2021 February. In 2012 April, the larger particles arrived. A few months later, in the summer of 2012, the small particles arrived, in a wide pattern distributed mainly at the orbit radii. The small particles compose the wide tail of the trail, dispersing wider even after the other particles had already left the southern node.

After completing one revolution past the outburst point, the dust particles arrived at the northern node at the beginning of 2014. The medium sized particles arrived first, followed by the larger particles immediately thereafter. The small particles arrived at the 2007 outburst point considerably later, towards the end of 2014.

In 2014 October, the dust particles left the southern node. The long tail of the trail with small particles was moving outside of the orbit radii. When small particles were leaving the vicinity of the southern node, they were ∼0.3 AU farther in the Z heliocentric axis.

In 2016 October, the majority of dust particles left the northern node 2007 outburst point, leaving behind only the small particles.

The larger and medium-sized dust particles arrived again to the northern node two revolutions after the 2007 outburst, in 2020 June. Physically, at that time, the spearhead of the tail was located approximately 0.1 AU further in the orbit radii. The small particles arrived later, in 2021 March; when they arrived, the trail was spatially more near the 2007 outburst point compared to when the larger particles arrived. The density of small particles is low when they start populating the 2007 outburst point in 2021 March.

4.2 Observations at the southern orbit node 2013 and 2014

We made three observing runs for the southern node. The dust had travelled to the southern node over a year before the observations started.

Our first observations of the dust were made at the Siding Spring Observatory in 2013 February. The modelling results show that all particle sizes modelled were still present in the dust trail (Figs 2–5). The observed part of the dust trail was already situated towards the end part of the trail.

The second observation made in 2013 August showed a dust trail, which according to our model had still all sized particles present (Figs 6–7).

The third series of observations was performed in 2014 February, and it showed only medium and small particles present in the dust trail (Figs 8–9).

4.3 Observations near the 2007 outburst point at the northern orbit node 2014 and 2015

The dust had travelled to the 2007 outburst site for over six months before the first observation. Observations started in 2014 August from the Auberry Sierra Remote Observatory. All particle sizes were present in the cometary dust trail (Figs 10–11).

Observations were continued at the Auberry Sierra Remote Observatory and at the New Mexico Skies observatory in 2014 September, when the comet itself was located on top of the dust trail as seen from Earth. All particle sizes were present during the observation with the comet itself (Figs 12–13).

In 2014 September, the Hankasalmi Observatory, Finland, also joined observations (Figs 14–15).

Starting from 2014 December the trail became brighter which made it possible to interpret the observations without image subtraction. All particle sizes were present in the vicinity of the 2007 outburst point. Additionally, mosaic images from the dust trail were made at the Hankasalmi observatory in 2015 February (Figs 16–21).

2015 August observations from Auberry Observatories showed all particle sizes (Figs 22–23).

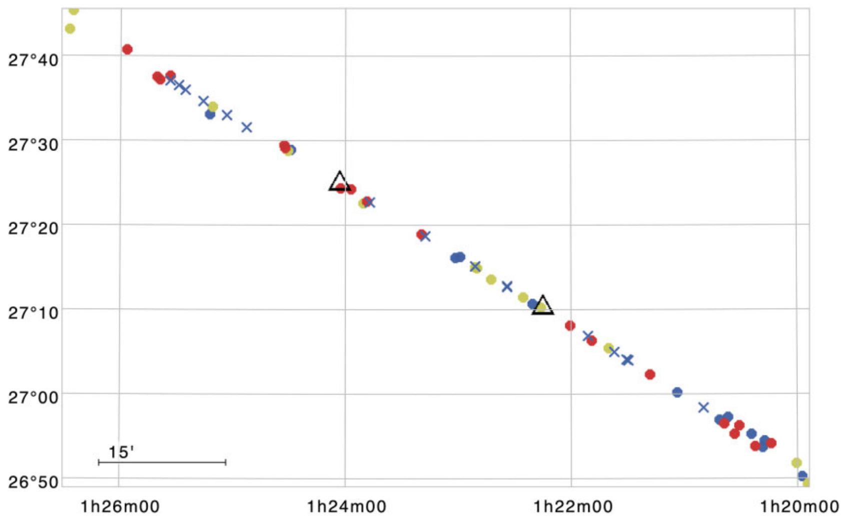

Figure 19. Modelling of the observation 2015 February 15 (M14). The X-axis shows RA and the Y-axis DEC. Blue: SPs. Yellow: MPs. Red: BPs. Black triangles: start and end observed positions of the trail. Particles ejected towards the Sun are marked with crosses.

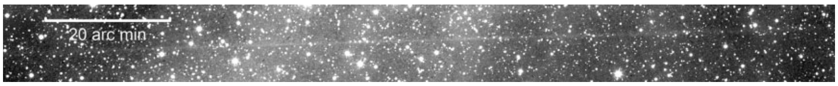

Figure 20. Observation of the trail as seen in 2015 February 15 (M14). Without image subtraction.

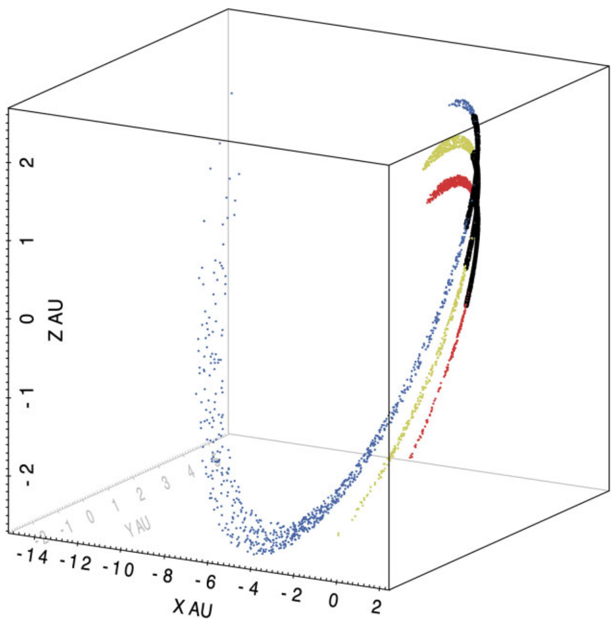

Figure 21. Modelling results for the time of the observation made in 2015 February 15 (M14). Here we show a complete modelled dust trail. The 40° RA sections of the trail are coloured here by black. The particles are shown in the ICRF coordinates XYZ. Blue: SPs. Yellow: MPs. Red: BPs. In order to fully demonstrate all particle populations, we have applied offset Z = 0.5 to the blue particles and offset Z = −0.5 to the red particles.

Last observations of the trail were made in 2015 October from Auberry. Then only small and medium-sized particles were present at the 2007 outburst point. The density of medium-sized particles was decreasing by a factor of ∼0.7 and the small particles started dominating the 2007 outburst point (Figs 24–25).

4.4 Observing campaign 2020–2021

The search of the trail was initiated in 2020 September from the New Mexico Skies observatory. The small particles had not yet travelled to the vicinity of the 2007 outburst point. However, the big and medium-sized particles were present there. The search continued into 2020 October. While the small particles had not yet arrived, the medium and big sized particles were present with the increased density. No trail was visible even when using image subtraction technique.

A continued search of the trail was made again in 2021 March from New Mexico Skies observatory. The small particles started populating the 2007 outburst point, but not with notable density. The big and medium-sized particles were present with even higher density compared to 2020 September and October. The dust trail was likely low in the sky (∼20–30° in altitude) since it was not visible with image subtraction technique in the observations.

Physically, the trail was even further away from the original 2007 outburst point than during the successful observation time, in 2015 February, and is expected to remain as such in 2022 February predictions.

In 2021 August, all particles were present at the 2007 outburst point, but the density of the small particles was not yet high (see supporting figures in Supplementary Material).

The comet itself was near the trail in August and at the beginning of 2021 September. The comet has crossed the narrowest part of the trail in the middle of 2021 August. In Supplementary Material the comet is plotted on top of the modeled trail section for 2021 September 6. The convergence point movement in the sky is also shown.

4.5 Predictions for 2022

The density of small particles is not expected to increase significantly until well into 2022 (Figs 26–28). The physical dust trail is predicted

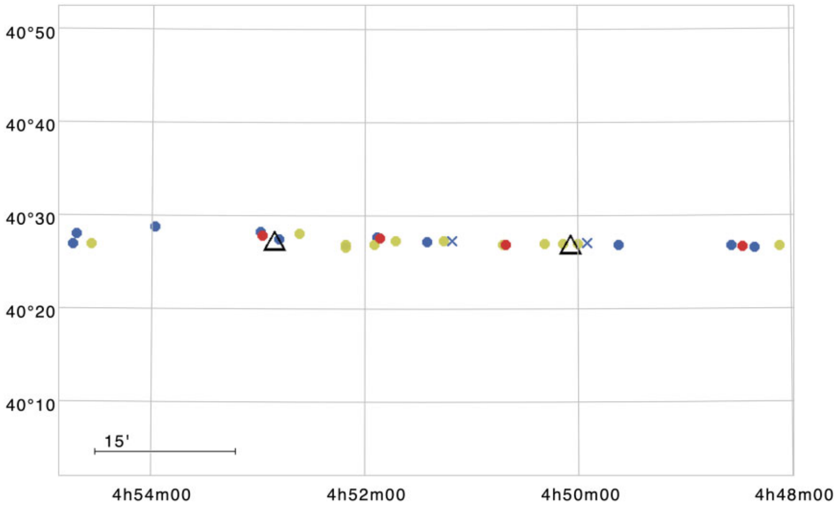

Figure 22. Modelling versus observation made in 2015 August 18 (M10). The X-axis shows RA and the Y-axis DEC. Blue: SPs. Yellow: MPs. Red: BPs. Black triangles: observed start and end positions of the trail. Particles ejected towards the Sun are marked with crosses.

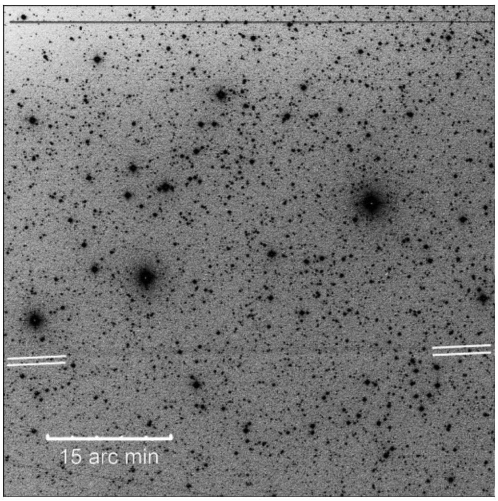

Figure 23. Observation 2015 August 18 (M10). Image subtraction. Darker trail is M10.

to move towards the original 2007 outburst point. The width of the trail seen from Earth in February and March of 2022 will be comparatively similar to the 2015 February observations. The particle density is expected to be comparatively similar as well. All particle sizes will be present in the trail near the 2007 outburst point.

The brightness of the 2015 February trail was bigger than our spherically symmetrical or towards the Sun outburst modelling achieve. Alternative explanation of the increase in actual brightness of the trail could be ejection of additional material from the comet relative to what is assumed in our model, e.g. during or after to the time of the 2007 outburst.

In 2022 August, the density of big particles is starting to decrease. The trail takes up the space of considerably more than a full orbit length and includes the dispersed tail in 2022. In Supplementary Material we show the visualization of hourglass pattern in both, near the 2007 outburst point and at the southern orbit node. The modelling of the dust trail in 2022 August are shown in Fig. 29.

The dust trail should be within the reach for even modest telescopes in 2022. However, image subtraction techniques are needed when observing with a small telescope (Alard 2000). We estimate that the brightness of the two-revolution dust trail is nearly similar to or brighter than that during the 2013 observations of the dust trail in the far side node, when the surface brightness was 26.8 mag arcsec^{-2} and the phase angle was 15.56° (Lyytinen et al. 2013b). The brightness value was also measured, when dust trail was directly observed during 2015 observations near the 2007 outburst point in the northern hemisphere (Lyytinen et al. 2015). We further estimate that the two-revolution dust trail is less bright, than that surface brightness of 25 mag arcsec^{-2} when the phase angle was 21.45°. The brightness estimates provided here are based on comparing the modelled trail widths and the densities for the entire range of modelled particles. The phase angles difference and therefore changed albedo causes 20 per cent brightness increase for 2013 February observations compared with 2015 February observations (Kolokolova et al. 2004). There is however uncertainty of the reason for the brightness increase in 2015 February trail (as discussed above) and that requires further investigations for predictions.

When accounting for the solar radiation pressure effects and modelled particle size distribution, the measurements we made by direct observing are consistent with the modelling results. The trail position is in good agreement with the modelling and the narrowest points of the trail are in good agreement with the spherically symmetric particle ejection model.

There can be other non-gravitational and non-regular radiation pressure effects acting on the particles, such as seasonal type radiation effects, which can slow down the particles even more than our modelling can account for.

We have not directly observed or modelled such effects at this juncture, because the behaviour of the particles in the dust trail suggests that they are influenced mainly by solar radiation pressure and Jupiter's gravitational effects. Future observations are expected to shed more light on the magnitude of such secondary effects.

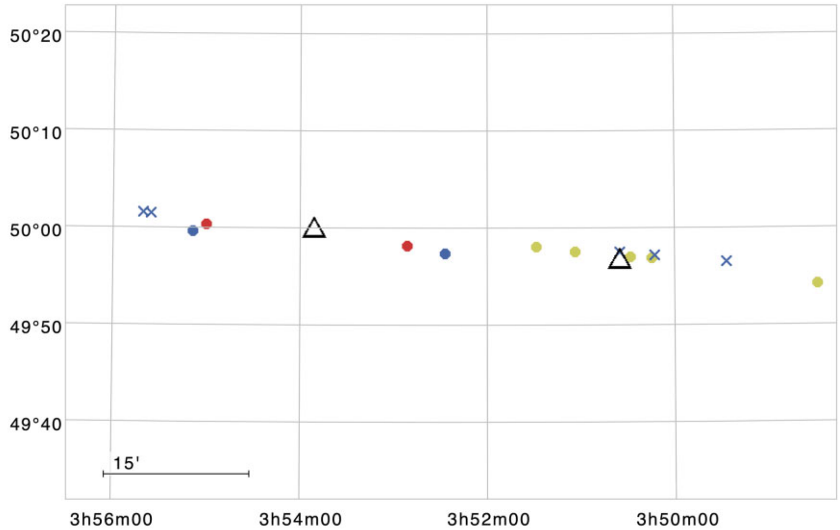

Figure 24. Modelling of observation 2015 October 24 (M11). The X axis shows RA and the Y axis DEC. Blue: SPs. Yellow: MPs. Red: BPs. Black triangles: start and end observed positions of the trail. Particles ejected towards the Sun are marked with crosses.

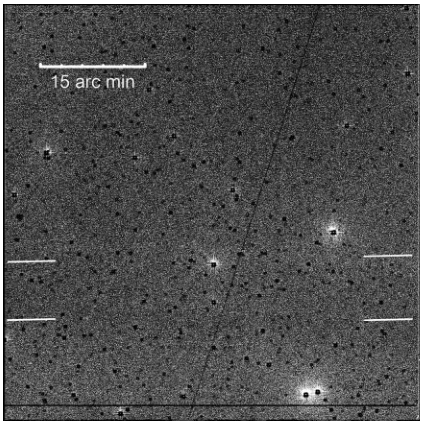

Figure 25. Observation 2015 October 24 (M11). Image subtraction. The upper trail is M11.

5 FUTURE OBSERVATIONS

Our prediction with the particles' calculated coordinates of the centre of the trail section nearest to the 2007 outburst point for years 2021 and 2022 are shown in Supplementary Material.

Direct observations in the vicinity of the hourglass centre and the dust trail in 2022 and later may likely provide further information about the following:

(i) symmetry conditions and exact mechanism of the 2007 outburst,
(ii) possible dispersion of material in interplanetary space,
(iii) characterizing non-regular radiation pressure effects, such as seasonal type radiation effects to the particles, as it requires longer time span of observations than a few revolutions,
(iv) particle size distribution evolution in the dust trail.

Observations can aid in calculating the following parameters:

(i) the extent of the phenomena measured in time,
(ii) position of the dust trail,
(iii) width of the trail and width of the hourglass centre,
(iv) the brightness evolution of the dust trail in time.

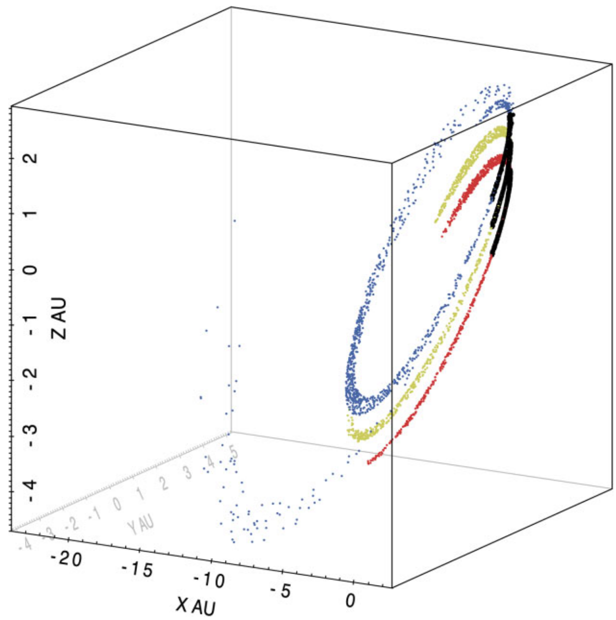

Figure 26. Modelling of the predicted trail for 2022 February (2022–02-15T12:00:00) (F7). The section highlighted is modelled in more detail near the 2007 outburst point. Blue: SPs. Yellow: MPs. Red: BPs. Black circles: 2007 outburst point centered 40° RA window. Particles are shown in the ICRF coordinates XYZ. In order to fully demonstrate all particle populations, we have applied offset Z = 0.5 to the blue particles and offset Z = −0.5 to the red particles.

The density of particles in the trail will be lower, density for all particles in 2022 February prediction is ∼0.7 times the density in 2015 February modelling results (Figs S1, S2). Phase angle was 21.45° in 2015 February and 21.25° in 2022 February. Albedo of particles is dependent on the phase angle. Phase angles are on all occasions in this study between 12° and 25°. Albedo difference is here below 10 per cent in the least-squares fit to the data presented by Kolokolova et al. (2004).

Upon discovery on 1892 November 6 by Edwin Holmes, comet 17P/Holmes also underwent an outburst at that time that led to the

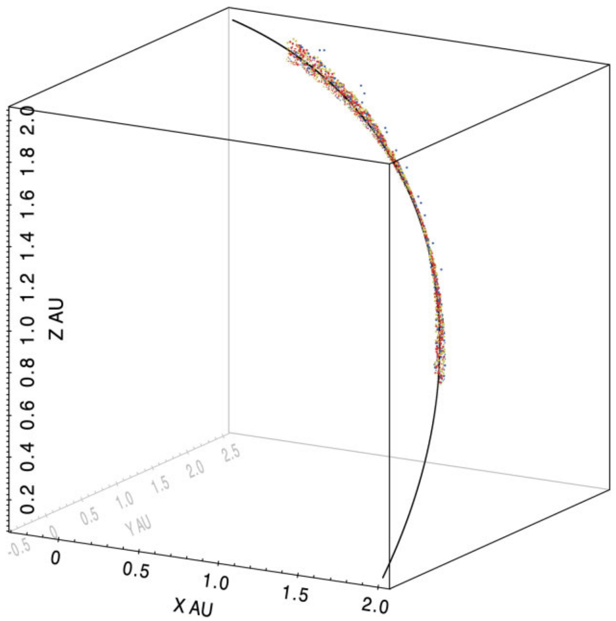

Figure 27. Prediction of the dust trail in 2022 February (2022–02-15T12:00:00) (F7) near the 2007 outburst point. Marked in the figure is the 17P/Holmes orbit at 2007 outburst event, the modelled 2015 February trail (2015–02-14T12:00:00) (M13) and 0.01 AU further away the modelled 2022 February trail. The particles are shown in the ICRF coordinates XYZ.

discovery of the comet (Hsieh et al. 2010). It could be beneficial to model that outburst in more detail as well as to examine if some effects of the 1892 outburst could be still observable. In a longer interval, non-regular radiation effects can become more prominent.

If the previously generated dust trails are visible in the future, they will be deflected even farther away. It is not clear if they are sufficiently bright for direct observations.

According to our model, there will be no further loss of the particles after the initial mass-loss from the trail has occurred. If there is a loss, vanishing, or break up of the particles, not accounted for in our model, the phenomenon might be dimmer than expected. In the previous observations we have not identified any substantial brightness decrease that has resulted from the loss of material. This is however difficult to measure, because the outburst mechanism is not known in such detail, and it is difficult to determine optical depth test particles that are consistent with both model and observations.

In 2022 the dust will be observable in visible light. While dust particles are not bright in the near-infrared spectrum, they could occasionally also be observable, where they will become brighter. Dust particles will be observable also in the mid-infrared spectrum.

The interaction of light and particles in the comet's trail is currently a subject of our investigation and the results will be reported in a separate later publication.

6 CONCLUSIONS

This paper describes a comprehensive dust trail particle model that was built upon the previous model developed by Lyytinen (1999), Lyytinen & Van Flandern (2000), and Lyytinen et al. (2001). The improved model includes multiparticle Monte Carlo modelling and was enhanced by including the solar radiation pressure effects, gravitational disturbance caused by Venus, Earth and Moon, Mars, Jupiter and Saturn, and gravitational interaction of the dust particles with their parent comet. We use this model to describe the dust trail evolution of the comet 17P/Holmes for a full time period since the spectacular outburst in 2007 October.

For the first time, the hourglass pattern of a comet trail has been observed, and modelling was used to explain it. We found that spherical symmetry of the ejected particles is responsible for producing the hourglass pattern (versus a purely theoretical case when all particles are ejected towards the sun).

The spherically symmetric outburst model is not able to explain the concentration of particles implied by the sharp increase in brightness of the trail near the outburst location in 2015 February observations. When we add the towards the Sun model, it brings small particles directly to the centreline of the trail, but not sufficiently close.

When comparing the 2013 February model versus observations, the spherically symmetric model gives a better agreement. Towards the Sun ejected particles concentrate on the centreline of the trail, which results in an overly bright trail compared to what was observed.

In all cases where the hourglass pattern of the trail was observed, it also resulted from our model with spherically symmetric modelling

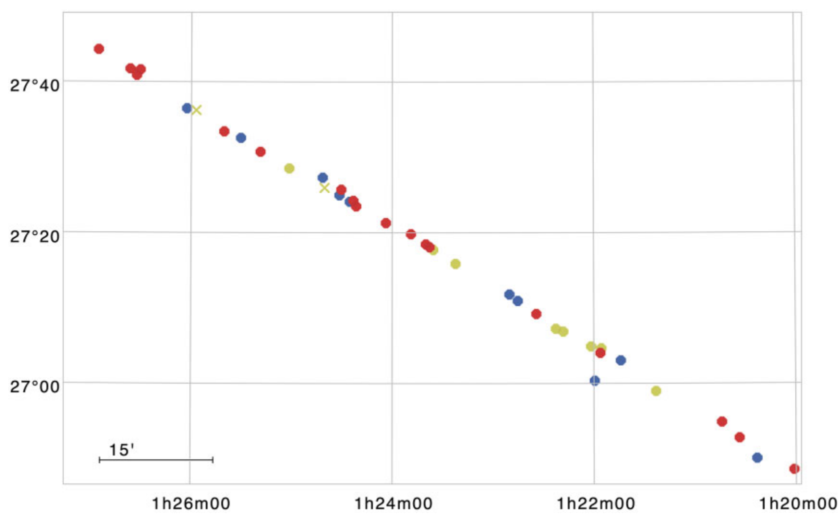

Figure 28. Modelling of the dust trail in 2022 February (2022–02-15T12:00:00) (F7). The X-axis shows RA and the Y-axis DEC. Blue: SPs. Yellow: MPs. Red: BPs. Particles ejected towards the Sun are marked with crosses.

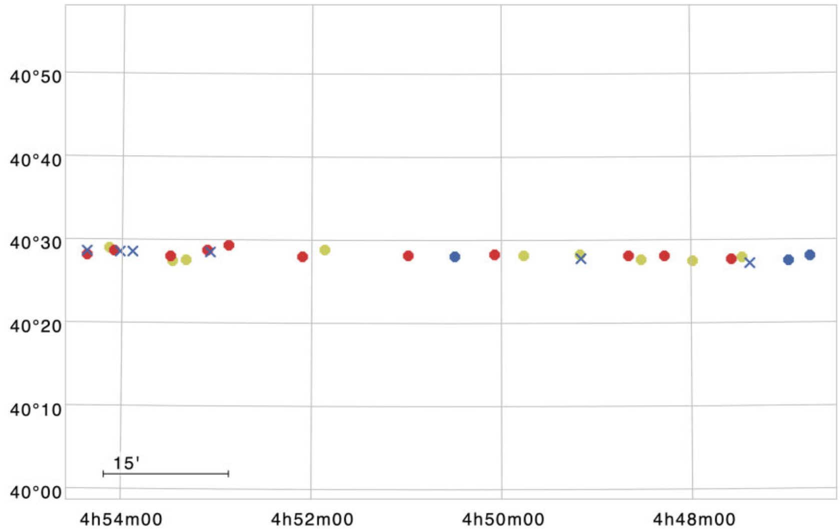

Figure 29. Modelling of the dust trail in 2022 August (2022–08-18T12:00:00) (F9). The X axis shows RA and the Y axis DEC. Blue: SPs. Yellow: MPs. Red: BPs. Particles ejected towards the Sun are marked with crosses.

of the outburst. Towards the Sun ejected particles do not contribute to the creation of a hourglass pattern, instead they produce a sharp concentrated line of particles on the trail centreline.

To support our model, we have conducted ground-based telescopic observations of the dust trail when the particles converge in any of the two common nodes (in the near-side common node or the far-side common node). The observations were done in visible light and span for a significant period, from 2013 to 2015. The new improved model was successfully validated by directly comparing the dust trail particle observations with the modelled particle distributions during a time-span extending for several years. The modelled trail position, width and narrowest point determination of the trail were found to be in excellent agreement with the observations.

Further to this, the improved model was used to constrain future evolution of the dust trail by providing predictions for the trail position and visibility. At present, the two-revolution dust trail is twice as dispersed temporally, and at the same time it is dimmer than when the particles had travelled one revolution around the Sun. However, near the 2007 outburst point, the apparent observable radial dispersion is not significantly larger.

The dust trail is expected to be deflected further away by approximately 0.01 AU in March of 2022, mainly due to the gravitational disturbance of Jupiter, and solar radiation pressure to some extent. The distance varies slightly, and the trail was located a few hundredths of AU farther away in February of 2021.

We predict that the evolved dust trail of the comet 17P/Holmes should be visible with even modest telescopes in 2022. Observing the dust trail in 2022, or later, will provide even more insight into understanding this phenomenon. Continuous future observations will also enable further modelling development since long-term ground truth information is essential for validating and improving the models.

ACKNOWLEDGEMENTS

This work was supported, in part, by the Academy of Finland project no. 325806 (PlanetS). The authors express deep gratitude and dedication to Esko Lyytinen, in particular, for initiating this research and for putting in place effective collaboration under the umbrella of the Ursa Astronomical Association and the Finnish Fireball Network. Intense collaborative work with Esko allowed us to provide a comprehensive representation of the ideas earlier discussed with Esko in the form of personal communications. We are grateful to Pekka Lehtikoski for his contribution to the programming of the mathematical model. We thank Jérémie Vaubaillon for insightful comments and discussion, which helped us to improve the earlier version of this paper. We thank Jorma Ryske for his enthusiastic observations of the trail in 2022 February and March and for confirming the observability and position of the trail as described and predicted in this study. This research made use of TOPCAT for visualization and figures (Taylor 2005).

DATA AVAILABILITY

The data underlying this study are included in the article and supporting information. TOPCAT files containing the output modelling data used for visualization can be shared on a reasonable request to the corresponding author.

CONFLICT OF INTEREST

The authors have no conflicts of interest to declare that are relevant to the content of this article.

REFERENCES

Alard C., 2000, A&AS, 144, 363
Altenhoff W.J., Kreysa E., Menten K.M., Sievers A., Thum C., Weiss A., 2009, A&A, 495, 975
Burns J.A., Lamy P.L., Soter S. 1979, Icarus, 40, 1
Casali M. et al., 2007, Min. Plan. Elec. Circ., 2007–U69
Dumoulin C. 1994, Celest. Mech. Dyn. Astron., 59, 73
El-Houssieny E.E., Nemiroff R.J., Pickering T.E., 2010, Astrophys. Space Sci., 330, 19
Giorgini J.D., 2021, Horizons On-Line Ephemeris System. Jet Propulsion Laboratory, Pasadena
Hsieh H.H., Fitzsimmons A., Joshi Y., Christian D., Pollacco D.L., 2010, MNRAS, 407, 1784
Ishiguro M. et al. 2013, ApJ, 778, 19
Ishiguro M. et al. 2016, ApJ, 817, 77

Kolokolova L., Hanner M. S., Levasseur-Regourd A. C., Gustafson B. Å. S., 2004, in Festou M., Keller H. U., Weaver H. A., eds, Comets II, Vol. 745. University of Arizona Press, Tucson, p. 577
Kossacki K. J., Szutowic S., 2011, Icarus, 212, 847
Lin Z. Y., Lin C. S., Ip W. H., Lara L. M., 2009, AJ, 138, 625
Landgraf M., Baggaley W.J., Grün E., Krüger H., Linkert G., 2000, J. Geophys. Res.: Space Phys., 105, 10343
Lyytinen E. J., Van Flandern T., 2000, Earth Moon Planets, 82, 149
Lyytinen E., 1999, Meta. Res. Bullet., 8, 33
Lyytinen E., Lehto H. J., Nissinen M., Jenniskens P., Suomela J., 2013, Centr. Bur. Electron. Telegrams, 3633
Lyytinen E., Nissinen M., Lehto H. J., 2013, J. Intern. Meteor. Organ., 41, 77
Lyytinen E., Nissinen M., Oksanen A., 2015, Astron. Telegrams, 7062
Lyytinen E., Nissinen M., Van Flandern T., 2001, J. Intern. Meteor. Organ., 29, 110
Lyytinen E., Nissinen M., Lehto H. J., Suomela J., 2014, Centr. Bur. Electron. Telegrams, 3969
Maisonobe L., Pommier V., Parraud P., 2010, ICATT 2010, ESAC Madrid
Marsaglia G. Ann., 1972. Ann. Math. Stat., 43, 645
Muller M. E., 1959. Comm. Assoc. Comput. Mach., 2, 19
Montalto M., Riffeser A., Hopp U., Wilke S., Carraro G., 2008, A&A, 479, L45
Nissinen M., Gritsevich M., Oksanen A., Suomela J. 2021a. LPI Contrib., 2609, 6010
Nissinen M., Gritsevich M., Oksanen A., Suomela J. 2021b. Dust Trail Observations of Comet 17P/Holmes and Predictions for 2021-2022, European Planetary Science Congress, 13–24 Sep 2021, EPSC2021–86
Park R., Folkner W., Williams J., Boggs D. 2021, AJ, 161, 105
Reach W. T., Vaubaillon J., Lisse C. M., Holloway M., Rho J., 2010, Icarus, 208, 276
Sekanina Z., 2009, Intern. Comet Quart., 5
Sposetti S. et al., 2007, Min. Plan. Elec. Circ., 2007
Taylor M. B. 2005. in Shopbell P. L., Britton M. C., Ebert R.eds, ASP Conf. Ser. Vol. 347, Astronomical data analysis software and systems XIV. Astron. Soc. Pac., San Francisco, p. 29
Vaubaillon J., Colas F., Jorda L., 2005, A&A, 439, 751
Zubko E., 2013, Earth Planets Space, 65, 2

SUPPORTING INFORMATION

Supplementary data are available at *MNRAS* online.

Supplementary Material Holmes MNRAS revised March 2022.pdf

Please note: Oxford University Press is not responsible for the content or functionality of any supporting materials supplied by the authors. Any queries (other than missing material) should be directed to the corresponding author for the article.

APPENDIX: LIST OF SYMBOLS

β = ratio of radiation pressure to gravity
μ = gravitational parameter of the Sun
μ' = Solar radiation pressure affected gravitational parameter of the Sun effective to particle
ν_{ex} = ejection velocity x component
ν_{ey} = ejection velocity y component
ν_{ez} = ejection velocity z component
v_{0x} = Particle's velocity at the start location (x component)
v_{0y} = Particle's velocity at the start location (y component)
v_{0z} = Particle's velocity at the start location (z component)
v_x = Particle's velocity x component after ejection speed is added
v_y = Particle's velocity y component after ejection speed is added
v_z = Particle's velocity z component after ejection speed is added
x_{earth} = Earth's location x component in the International Celestial Reference Frame (ICRF/J2000) standard celestial reference system
y_{earth} = Earth's location y component in the International Celestial Reference Frame (ICRF/J2000) standard celestial reference system
z_{earth} = Earth's location z component in the International Celestial Reference Frame (ICRF/J2000) standard celestial reference system
x_p = Particle's location x component in the International Celestial Reference Frame (ICRF/J2000) standard celestial reference system
y_p = Particle's location y component in the International Celestial Reference Frame (ICRF/J2000) standard celestial reference system
z_p = Particle's location z component in the International Celestial Reference Frame (ICRF/J2000) standard celestial reference system
x_g = Geocentric x component of the particle
y_g = Geocentric y component of the particle
z_g = Geocentric z component of the particle
α = Declination
θ = Right ascension

This paper has been typeset from a DOC file prepared by the author.